Protein Science (1996), *5*:1477–1489. Cambridge University Press. Printed in the USA.

X-ray crystallographic and mass spectrometric structure determination and functional characterization of succinylated porin from *Rhodobacter capsulatus*: Implications for ion selectivity and single-channel conductance*

MICHAEL PRZYBYLSKI,[1] MICHAEL O. GLOCKER,[1] UWE NESTEL,[2] VOLKER SCHNAIBLE,[1] MARTIN BLÜGGEL,[1] KAY DIEDERICHS,[2] JURGEN WECKESSER,[3] MICHAEL SCHAD,[4] ANGELA SCHMID,[4] WOLFRAM WELTE,[2] AND ROLAND BENZ[4]

[1] Universitat Konstanz, Fakultat fur Chemie, P.O. Box 5560M731, 78434 Konstanz, Germany
[2] Universitat Konstanz, Fakultat fur Biologie, P.O. Box 5560, 78434 Konstanz, Germany
[3] Universitat Freiburg, Institut fur Biologie II, Mikrobiologie, Schänzlestr. 1, 79104 Freiburg im Breisgau, Germany
[4] Universität Würzburg, Lehrstuhl fur Biotechnologie, Theodor-Boveri-Institut (Biozentrum), Am Hubland, 97074 Würzburg, Germany

(RECEIVED March 26, 1996; ACCEPTED May 2, 1996)

Abstract

The role of charges near the pore mouth has been discussed in theoretical work about ion channels. To introduce new negative charges in a channel protein, amino groups of porin from *Rhodobacter capsulatus* 37b4 were succinylated with succinic anhydride, and the precise extent and sites of succinylations and structures of the succinylporins determined by mass spectrometry and X-ray crystallography. Molecular weight and peptide mapping analyses using matrix-assisted laser desorption-ionization mass spectrometry identified selective succinylation of three lysine-ϵ-amino groups (Lys-46, Lys-298, Lys-300) and the N-terminal α-amino group. The structure of a tetra-succinylated porin (TS-porin) was determined to 2.4 Å and was generally found unchanged in comparison to native porin to form a trimeric complex. All succinylated amino groups found in a mono/di-succinylated porin (MS-porin) and a TS-porin are localized at the inner channel surface and are solvent-accessible: Lys-46 is located at the channel constriction site, whereas Lys-298, Lys-300, and the N-terminus are all near the periplasmic entrance of the channel. The Lys-46 residue at the central constriction loop was modeled as succinyl-lysine from the electron density data and shown to bend toward the periplasmic pore mouth. The electrical properties of the MS- and TS-porins were determined by reconstitution into black lipid membranes, and showed a negative charge effect on ion transport and an increased cation selectivity through the porin channel. The properties of a typical general diffusion porin changed to those of a channel that contains point charges near the pore mouth. The single-channel conductance was no longer a linear function of the bulk aqueous salt concentration. The substantially higher cation selectivity of the succinylated porins compared with the native protein is consistent with the increase of negatively charged groups introduced. These results show tertiary structure-selective modification of charged residues as an efficient approach in the structure–function evaluation of ion channels, and X-ray crystallography and mass spectrometry as complementary analytical tools for defining precisely the chemically modified structures.

Keywords: cation selectivity; charge at pore mouth; crystallography; mass spectrometry; porin ion channels; single-channel conductance; succinylated porin; succinylation sites

* Dedicated to Professor Dr. Richard R. Schmidt on the occasion of his 60th birthday.

Reprint requests to: M. Przybylski, Fakultat fur Chemie, Universitat Konstanz, P.O. Box 5560M731, 78434 Konstanz, Germany; e-mail: michael.przybylski@uni-konstanz.de.

Abbreviations: BrCN, cyanogen bromide; MS-porin, mono/di-succinylated porin; TS-porin, tetra-succinylated porin; ESI-MS, electrospray mass spectrometry; HCCA, α-cyano-4-hydroxycinnamic acid; MALDI-MS, matrix-assisted laser desorption ionization mass spectrometry; nS, nano Siemens; OM, outer membrane; PDMS, plasma desorption mass spectrometry; TFA, trifluoro-acetic acid; TPCK, Tosyl-phenylalanyl-chlormethyl-keton.

Gram-negative bacteria protect themselves against bactericidal substances by the outer membrane, which envelops entirely the vulnerable plasma membrane, creating an additional aqueous compartment, the periplasmic space. The OM is asymmetrically composed of a lipopolysaccharide monolayer toward the medium and a phospholipid monolayer toward the periplasmic space (Rietschel et al., 1988). Among the Gram-negative bacteria, there is considerable variation of the lipopolysaccharide component. Porins, which form the major protein component of the OM, form aqueous channels that allow the permeation of small molecules up to a mass of, typically, 600 for enteric bacteria (for reviews see Benz, 1988; Welte et al., 1995).

The structures of five bacterial porins (four general diffusion channels and one specific porin) have been determined by X-ray crystallography: *Rhodobacter capsulatus* (Weiss et al., 1991a, 1991b), *Escherichia coli* OmpF and PhoE (Cowan et al., 1992), *Rhodopseudomonas blastica* (Kreusch et al., 1994), and maltoporin from *E. coli* (Schirmer et al., 1995). All form trimers and consist of a 16–18-stranded β-barrel of similar overall shape and tilt of the β-strands. The connections are all between neighboring strands. All possess sharp β-hairpin loops on their periplasmic surface. The opposite barrel rim is rough due to an irregular termination of the β-strands and to loops of varying lengths connecting the neighboring strands on the external side. Although the porin structures are similar in the periplasmic half of the OM, they differ from each other in the medium-apposed half. In all porins, the third external loop is exceptionally large (approximately 45 amino acid residues). This segment folds in an extended conformation from the end of the fifth strand of the barrel rim along the inside barrel wall and back to the sixth strand. The free cross-section of the β-barrel cylinder of *R. capsulatus* porin, which is about 30 × 30 Å, is constricted to an opening of about 8 × 10 Å at the position of the third loop inside the barrel, which is roughly halfway through the channel (Fig. 1). The permeation of hydrated ions through this constriction loop may require transient stripping of part of their hydration shells (Weiss et al., 1991a).

The amino acid residues coating this central "constriction zone" or "eyelet" show a remarkably asymmetric charge distribution. Although the respective segments of the third loop are carrying acidic amino acids, the opposite barrel wall (near the center of the trimers) is coated with basic amino acid residues (Fig. 2). Reconstitution experiments with porin from *R. capsulatus* suggest that there is a link between the rate of permeation of cations through the porin and the number of acidic residues, as well as a similar link between anion permeability and basic residues (Benz et al., 1987; Weiss et al., 1991a; Cowan et al., 1992).

We have chemically modified porin from *R. capsulatus* 37b4 by introducing negative charges through succinylation with succinic anhydride. The effect of the succinylation on single-channel conductance and ion selectivity was studied by electrical measurements after reconstitution into lipid bilayer membranes. The molecular structures of the succinylated porins were characterized by direct molecular mass determination using MALDI-MS, which showed the selective introduction of up to four succinate groups; their localization (three lysine residues and the N-terminal α-NH_2-group) was identified by mass spectrometric peptide mapping analyses following proteolytic degradation, and by sequence identification of proteolytic peptides isolated by HPLC. The modified proteins crystallized isomorphically to the native protein so that the crystal structure and electron density map allowed the comparison of the structures by difference maps. The changes in the electrical properties are discussed in this study in view of the structures of the succinylated porins.

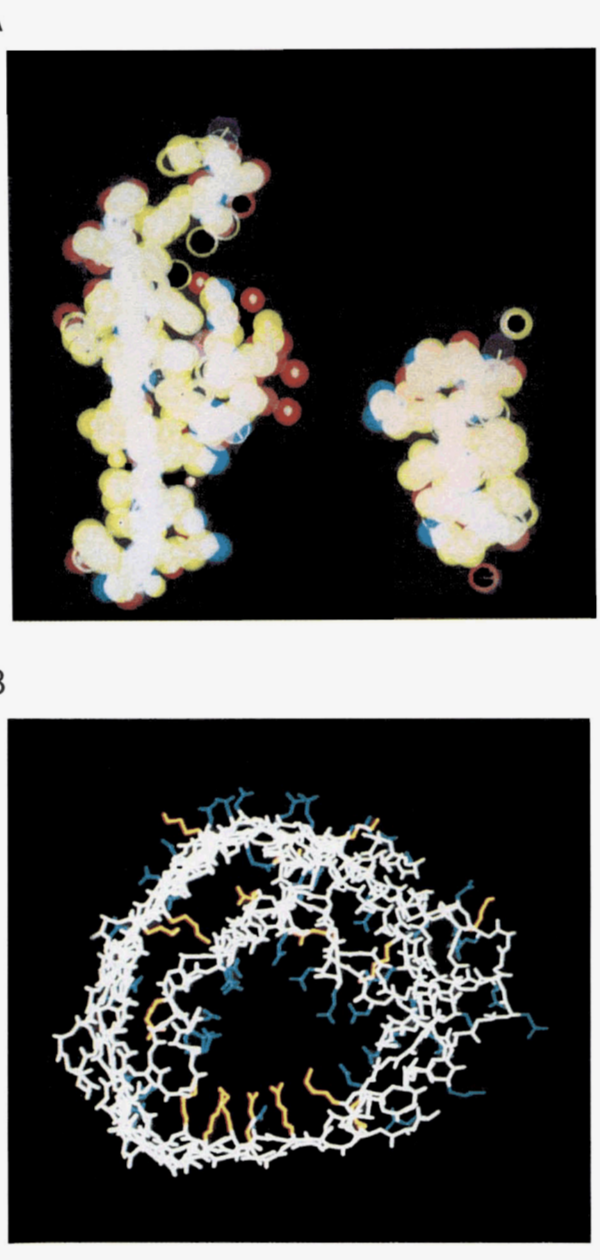

Fig. 1. A: Slab through a porin monomer along a plane spanned by the threefold axis of the trimer and a vector pointing from this axis to the center of the constriction site. The third loop, attached to the peripheral barrel wall, creates the constriction site. Colors used are white for peptide backbone atoms; red for side-chain oxygen; blue for side-chain nitrogen. **B:** View of the porin monomer along the threefold axis from the periplasmic side. The scheme shows the backbone atomic bonds in white, the acidic residues in blue, and the basic residues in orange, illustrating the strong charge asymmetry across the constriction site.

```
1           11          21          31          41
EVKLSGDARM GVMYNGDDWN FSSRSRVLFT MSGTTDSGLE FGASFKAHES
51          61          71          81          91
VGAETGEDGT VFLSGAFGKI EMGDALGASE ALFGDLYEVG YTDLDDRGGN
101         111         121         131         141
DIPYLTGDER LTAEDNPVLL YTYSAGAFSV AASMSDGKVG ETSEDDAQEM
151         161         171         181         191
AVAAAYTFGN YTVGLGYEKI DSPDTALMAD MEQLELAAIA KFGATNVKAY
201         211         221         231         214
YADGELDRDF ARAVFDLTPV AAAATAVDHK AYGLSVDSTF GATTVGGYVQ
251         261         271         281         291
VLDIDTIDDV TYYGLGASYD LGGGASIVGG IADNDLPNSD MVADLGVKFK F
```

Fig. 2. Amino acid sequence of porin from *R. capsulatus*. Lysine residues are boxed; the sequence comprising the third channel constriction loop is shaded.

Results

Mass spectrometric structure identification of succinylated porins

Native porin was subjected to succinylation with approximately 15- and 100-fold molar excesses of succinic anhydride for 60 min at 25 °C, ca. pH 6.5, at conditions that were established previously to provide selective N-acylation at lysine-ϵ-amino groups and the N-terminus, respectively (Nielsen et al., 1990; Suckau et al., 1992). The modified proteins were dialyzed against crystallization buffer and purified by FPLC on Q-sepharose. The succinylation did not lead to dissociation of the native trimer complex of porin, in accordance with the tertiary structure-selective acylation conditions of surface-accessible lysine residues (Glocker et al., 1994), and the protein derivatives showed a slight increase in the apparent mass by SDS-PAGE.

Precise molecular mass determinations of two succinylated porins were obtained by MALDI-MS, which, together with other "soft"-ionization methods such as ESI-MS and Cf-252-plasma desorption, have recently provided a breakthrough in the direct characterization of proteins and other biopolymers (Karas et al., 1991; Smith et al., 1991; Przybylski, 1995). MALDI mass spectra of the unmodified and two succinylated porins, obtained under acidic conditions in the solid crystalline matrix HCCA (leading to dissociation of the trimer complex), are compared in Figure 3A, B, and C. All three proteins yielded a consistent series of singly charged (protonated) molecular ions together with the doubly and triply charged ions (M^{2+}, M^{3+}). A molecular mass of 31,541 Da, in close agreement with the sequence molecular weight (M_r, 31,537 Da) of the monomer was determined for unmodified porin. The porin derivative modified with a 15-fold excess of succinic anhydride yielded a molecular mass of 31,684 Da, which, by calibration with the precisely defined molecular ions of trypsin, insulin, and BSA as internal standards, corresponds to a modification degree of 1.4 and hence to a mono- to disuccinylated porin; the higher modified porin, with a molecular mass of 31,941 Da, corresponds to the presence of four succinyl groups exactly (ΔM, 400 amu; Fig. 3B,C). Furthermore, the molecular ion peak widths for the succinylated porins compared with that of the unmodified porin (representing average-isotopes due to the time-of-flight analyzer employed), indicated a relatively high homogeneity and selective introduction of up to four succinyl-groups. Thus, the nar-

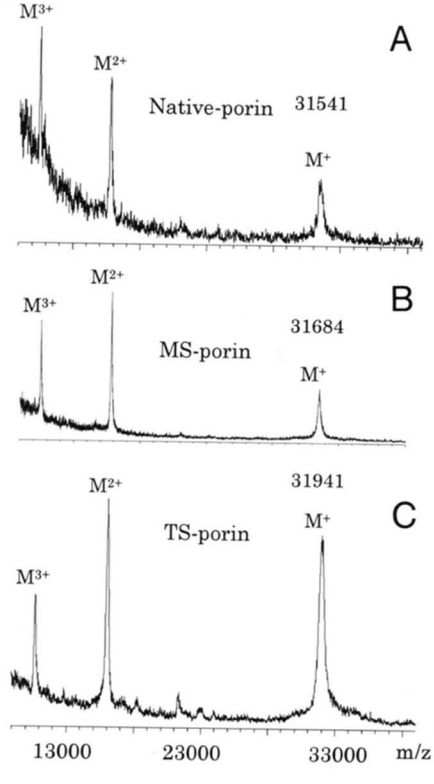

Fig. 3. MALDI-MS analysis of (**A**) unmodified (native porin), (**B**) MS-porin, and (**C**) TS-porin. Sample preparations for mass spectrometric determinations were performed by adding 1 μL of a 5-μg/μL solution of protein in crystallization buffer (see Materials and methods) to 19 μL of a matrix solution of HCCA in acetonitrile:0.1% TFA (2:1). Mass calibration was performed by using the precise average-isotope singly charged molecular ion signals of hen egg-white lysozyme, cytochrome *c*, trypsin, and BSA as internal standards.

row molecular ions in the spectrum of the native-like TS-porin suggested the presence of only very small amounts of tri- and penta-succinylated proteins (Fig. 3C). This result was in contrast to the much broader molecular ion signals observed for an approximately octa-succinylated, denatured protein prepared at more drastic reaction conditions with a 500-fold reagent excess (not shown). The selective modifications in the MS- and TS-porins was ascertained by the subsequent determination of specific succinylation sites and unsuccinylated lysine residues.

The complete structural characterization and identification of the succinylation sites of the MS-porin and TS-porin was obtained by (1) mass spectrometric peptide mapping of peptide mixtures after proteolytic degradation with BrCN and trypsin, (2) mass spectrometric analysis of peptide fragments isolated by HPLC, and (3) Edman sequence determination of the intact succinylated porins and of relevant isolated proteolytic peptides. Edman sequence analyses showed that the TS-porin was completely blocked, and, in the case of the MS-porin, provided a partial N-terminal sequence (EVKLS-) only with low sensitivity beyond background in comparison to native porin, indicating partial to complete (TS-porin) N_{α}-succinylation. Direct MALDI-MS peptide mapping analysis of BrCN fragments from MS-porin and TS-porin are compared in Figure 4 (see also Table 1). Molecular ions of three BrCN peptides were found that

Table 1. *Identification of proteolytic fragments and succinylation sites from unmodified and succinylated porins by BrCN and trypsin degradation*

Sequence/Lys residue[b]	m.w. calcul.[c]	MH^+ ions, m/z[c]			Sequence analysis[d]	Succinylated Lys residue
		Native porin	MS-porin	TS-porin		
BrCN fragments[a]						
(1-10)/3	1075	1060[e]	1159[e]	1159[e]	–	α-NH_2
(11-31)/–	2464[e]	2466	2465	2467		
(14-31)/–	2165	2170	2165	2167		
(1-31)/3	3541	3542	3542	3645	EVKL[f]	α-NH_2, K-3[f]
(32-72)/46, 69	4076	4077	4080/4175	4174	SGT	K-46[g]
(14-72)/46, 69	6274	6275	6275/6370	6371		K-46[g]
(73-134)/–	6477	6470	6488	6480		
(73-178)/138, 169	11097	11102	11104	11100		
(73-181)/138, 169	11462	11470	11469	11464		
(292-301)/298, 300	1124	1123	1125/1224	1324	VAD	K-298, K-300
Tryptic fragments[h]						
(1-9)/3	934	–	935/1034	1034	–[i]	α-NH_2
(1-26)/3	2979	–	3079	3079	–[i]	α-NH_2, K-3[f]
(4-9)/3	619	621	620	621		
(10-24)/–	1779	1779	1779	1780		
(10-46)/46	4100	4102	–	–		
(27-46)/46	2095	2095	–	–		
(27-69)/46	4344	4345	4445	4446		K-46
(42-62)/46[j]	2097	–	2199	2198	GASF[j]	K-46
(70-97)/69	3037	3037	3036	3039		
(98-110)/–	1406	1407	1407	1409		
(129-156)/138[j]	2788	2790	2791	2790	SVA[j]	
(170-191)/169, 191	2348	2347	2349	2349		
(192-198)/191, 198	737	737	738	738		
(199-208)/198	1173	1174	1172	1174		
(199-212)/198	1662	1663	1662	1665		
(213-230)/230	1797	1798	1799	1798		
(213-232)/230[j]	2030	2031	2030	2032		
(231-298)/230, 298	6821	6824	–	–		
(270-301)/298, 300[j]	3189	–	–	3390	DLGG[j,k]	K-298, K-300

[a] BrCN fragments identified from MALDI-MS peptide mapping, except for peptides (1-10) and (1-31), which were isolated by HPLC.
[b] Lys residues and N terminus contained in proteolytic peptide or involved in cleaved peptide bond.
[c] Average isotopic masses of BrCN peptides, homoserine-carboxylate unless otherwise noted.
[d] Edman sequence determination of HPLC-isolated peptide.
[e] BrCN peptide, homoserine-lactone (Fontana and Gross, 1986).
[f] Low amount of K-3 succinylation derived from sequenator background.
[g] K-69 succinylation excluded from tryptic cleavage at K-69/I-70 bond.
[h] From HPLC-isolated fragments obtained by digestion with TPCK-untreated trypsin.
[i] Peptide blocked at N terminus.
[j] Peptide resulting from chymotryptic cleavage; other chymotryptic fragments: (199-210); (202-210); (92-104).
[k] See Fig. 6C.

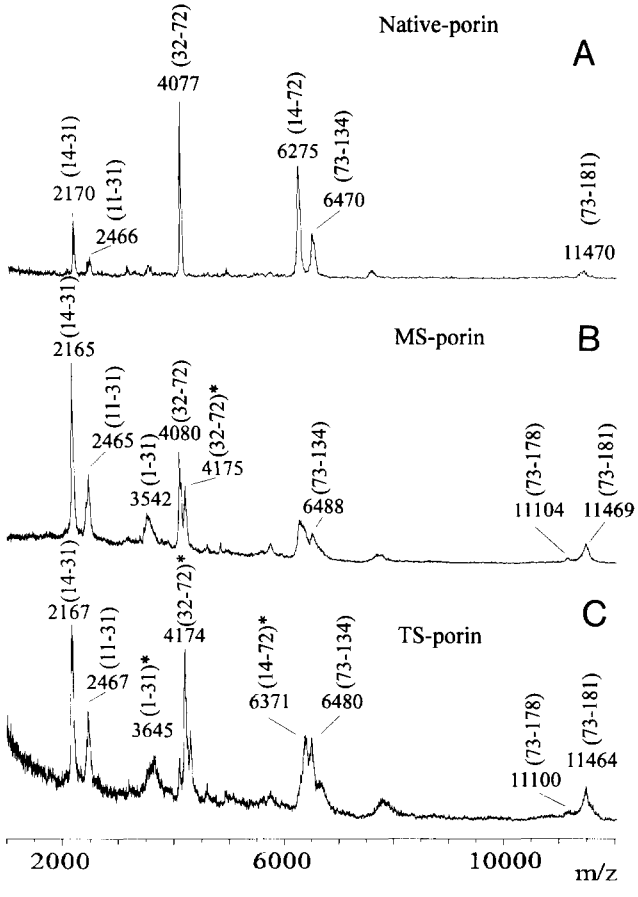

Fig. 4. MALDI-MS peptide mapping analysis of BrCN-peptides from (**A**) native porin, (**B**) MS-porin, and (**C**) TS-porin. A 1-μL aliquot of the BrCN reaction mixture was added to 19 μL of the HCCA matrix solution (see Materials and methods). Masses given represent the homoserine-carboxylate forms of BrCN-peptides (see Table 1 and text). Partial sequences are given in parentheses and are marked by an asterisk for succinylated peptides.

showed an increase in molecular mass by 100 amu each compared with the corresponding fragments from unmodified porin. Two of these peptides, (32–72) and (14–72), identified complete mono-succinylation at Lys-46 for TS-porin and partial Lys-46-succinylation in MS-porin (a modification at Lys-69 was excluded by analysis of tryptic peptides as shown below). Furthermore, mono-succinylation in the N-terminal part was confirmed by the peptide (1–31) in TS-porin (m/z 3,645), in contrast to the presence of some unmodified (1–31) in MS-porin. The succinyl-(1–31) peptide isolated from TS-porin by HPLC was amenable to Edman sequencing only at a very low background level, which indicated only a trace of alternative succinylation at Lys-3. This result was in agreement with the mass spectral identification of the HPLC-isolated BrCN peptide succinyl-(1–10), which was entirely blocked at the N-terminus (see Fig. 6A). Further possible succinylation sites at Lys-169 were ruled out by BrCN peptides (135–178) and (73–181), which were found unmodified both in the MS- and TS-porins. A large BrCN polypeptide fragment (182–291; M_r ca 12,500 Da) was not found by direct MALDI-MS analysis and could not be isolated by HPLC, probably due to its low solubility. However, the remaining two succinylation sites at Lys-298 and Lys-300 were identified by HPLC isolation, MALDI-MS and partial sequence analysis of the C-terminal peptide (292–301), which was unmodified in native porin and MS-porin, but was shifted by $\Delta M = 200$ amu in TS-porin (m/z 1,324; see Table 1).

Peptide fragments obtained by tryptic digestion were in complete agreement with the BrCN degradation in the determination of the four succinylation sites. Untreated trypsin containing additional chymotryptic activity was used in these experiments, as the intact porin structure was found difficult to digest with trypsin even after denaturation with urea (Schiltz et al., 1991) (however, results were confirmed by comparison with peptide mapping after digestion with TPCK-treated trypsin). HPLC separations of tryptic peptides from native porin are compared in Figure 5, and relevant lysine-containing peptide fragments (and cleavage sites at Lys residues) summarized in Table 1. Despite the multiplicity of proteolytic peptides, MALDI-MS of isolated fractions and partial sequence determinations provided complete primary structure coverage of succinylated porins. In addition to the blocked N-terminal peptide Na-succinyl-(1-9) in TS-porin (m/z 1,034), the succinylation at Lys-46 was ascertained by the modified peptide (27–69) and by the chymotryptic fragment (42–62), which provided a molecular mass due to mono-succinylation and the correct N-terminal sequence as well (GASF; see Fig. 6B). Also, Lys-298 and Lys-300 in TS-porin were found inaccessible

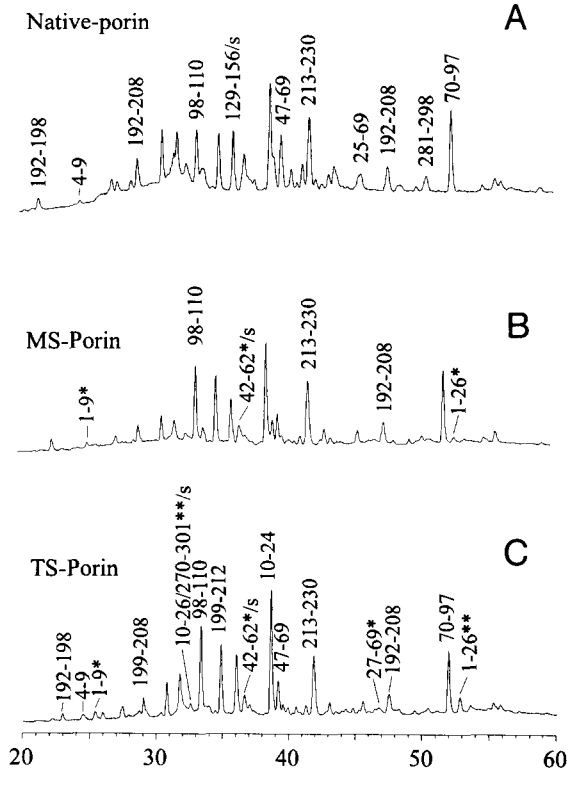

Fig. 5. HPLC separation of tryptic peptides from (**A**) native porin, (**B**) MS-porin, and (**C**) TS-porin. Proteins were digested with untreated trypsin, reaction mixtures injected on a 25 × 0.4 cm nucleosil-C8-column and eluted with a linear TFA/acetonitrile gradient, as described in Materials and methods. Succinylated peptides identified by MALDI-MS of isolated fractions, and by Edman sequence analysis are marked by asterisks "*" and by /s, respectively.

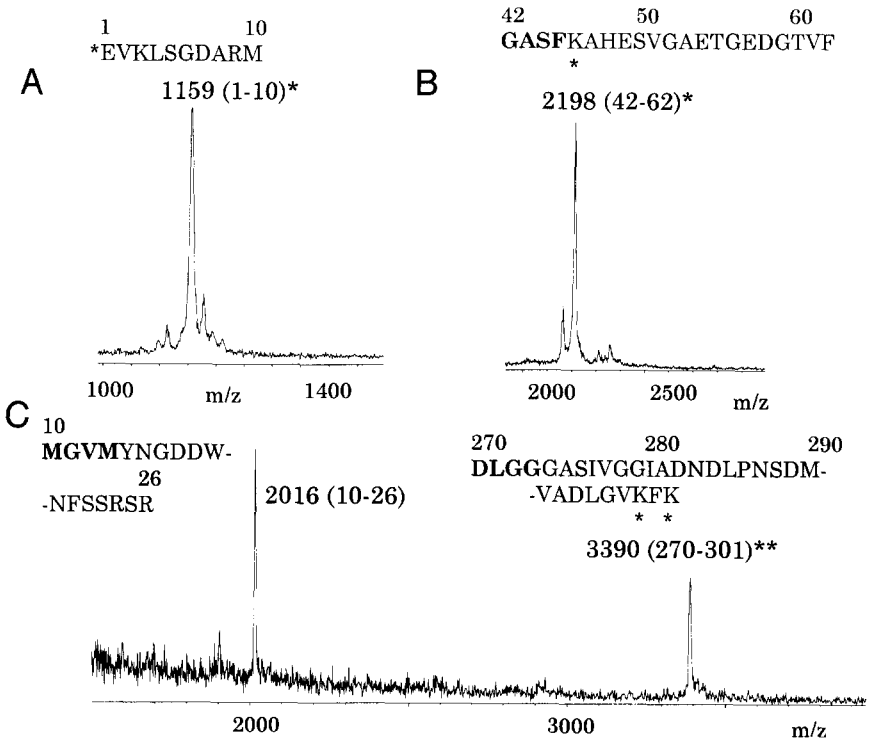

Fig. 6. MALDI mass spectra of succinylated peptide fragments isolated by HPLC after BrCN and trypsin digestion of TS-porin. **A:** Spectrum of BrCN peptide, Nα-succinyl(1-10), lactone form. **B:** Lys-46-εe-succinyl-(42-62). **C:** Mixture of peptides (10–26) and (Lys-298,300)-bis-succinyl-(270–301) (see Fig. 5 and Table 1). N-terminal residues determined by automated Edman degradation are indicated by bold letters.

to tryptic cleavage. These succinylation sites were identified by MALDI-MS and sequence analysis of the bis-succinylated chymotryptic peptide (270–301), despite the presence of an additional peptide (10–26) in the HPLC fraction (Fig. 6C). By contrast, other Lys-containing peptide fragments were found unmodified by MALDI-MS [e.g., (70–97), (129–157), (170–191), (199–208), and (213–230); (Table 1)]. In summary, these results ascertained the predominant succinylation at four specific amino groups in TS-porin (Lys-46, Lys-298, Lys-300, N-terminus) and partial N-terminal and Lys-46 succinylation in MS-porin. Furthermore, other lysine modifications were ruled out except for a low extent of succinylation at Lys-3 (and trace at Lys-69).

Single-channel conductance of succinylated porins

Single-channel experiments revealed that the MS- and TS-porins still had channel-forming activity, i.e., the channel-forming properties of the porin trimers remained intact on succinylation. The native and the succinylated porins had approximately the same channel-forming activity, indicating that if any change of the porin trimers had occurred at all, it was minor. Figure 7B (lower trace) shows a single-channel recording in the presence of TS-porin. The protein was added to a black diphytanoyl phosphatidylcholine/*n*-decane membrane at a concentration of about 20 ng/mL. A stepwise increase of the membrane conductance was observed after a delay of several minutes, probably caused by slow aqueous diffusion, reflecting the insertion of the TS-porin trimer into the membrane. Similar to the native porin trimers, the channels had a long lifetime (mean lifetime at least 5 min). The upper trace of Figure 7 shows a single-channel recording observed with native porin under otherwise identical

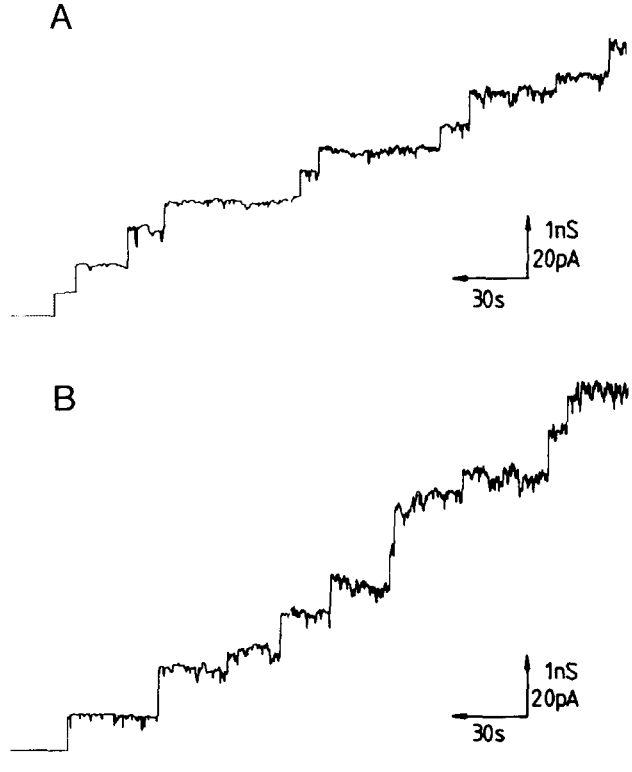

Fig. 7. Single-channel recording of diphytanoyl phosphatidylcholine/*n*-decane membranes in the presence of 20 ng/mL native porin (**A**) and TS-porin (**B**) from *R. capsulatus*. The aqueous phase contained in both cases 0.3 M KCl, pH 6. The applied membrane potential was 20 mV; $T = 20\,^{\circ}C$.

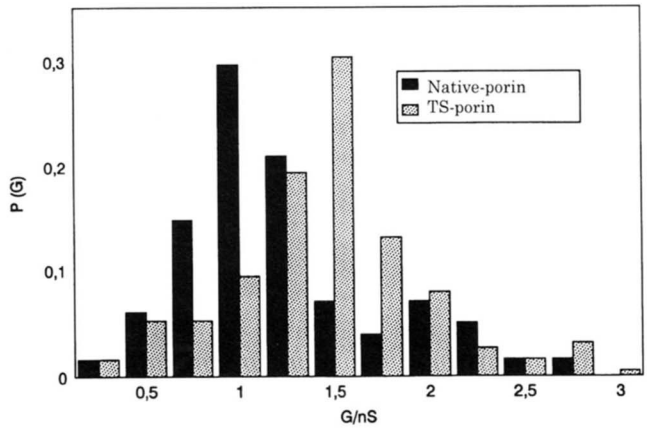

Fig. 8. Histogram of the probability $P(G)$ for the occurrence of a given conductivity unit observed with membranes formed of diphytanoyl phosphatidylcholine/*n*-decane in the presence of 20 ng/mL native porin and TS-porin. $P(G)$ is the probability that a given conductance increment G is observed in the single-channel experiments. It was calculated by dividing the number of fluctuations with a given conductance increment by the total number of conductance fluctuations. The aqueous phase contained 0.3 M KCl. The applied membrane potential was 20 mV; $T = 20\,°C$. The average single-channel conductance was 1 nS for 252 single-channel events (native porin) and 1.45 nS for 258 single events (TS-porin).

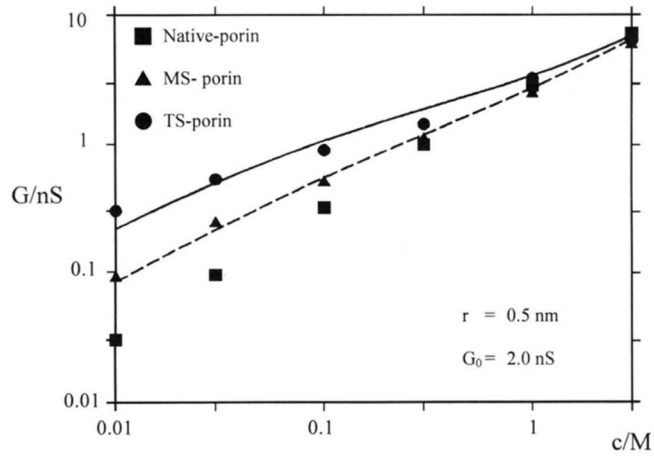

Fig. 9. Single-channel conductance of native porin (filled squares), MS-porin (filled triangles), and TS-porin (filled circles) as a function of the KCl-concentration in the aqueous phase. The solid line represents the fit of the single-channel conductance with a combination of Equations 1–3 by assuming a radius of the succinylated porin channel of 0.5 nm and 1.0 negative elementary charge ($q = -1.6 \cdot 10^{-19}$ As) localized at the channel mouth. The broken line represents a similar fit of the single-channel conductance by assuming the same radius and a negative elementary charge of 0.6 ($q = -0.96 \cdot 10^{-19}$ As) localized at the channel mouth. The single-channel conductance of the native poring is a linear function of the bulk aqueous concentration. c, concentration of the KCl-solution in M (molar); G, average single-channel conductance in nS.

conditions (0.3 M KCl). The comparison of the single-channel records indicated that the single-channel conductance was higher for the MS- and TS-porins than for native porin.

A histogram of the conductance fluctuations observed with native and TS-porin is shown in Figure 8 under the same conditions as in Figure 7 (0.3 M KCl). The TS-porin showed a single-channel conductance of 1.45 nS, whereas the native porin had only a conductance of 1.0 nS. Apart from this difference, the histograms for native and TS-porin were very similar, as demonstrated in Figure 8.

Single-channel conductance experiments were performed with native, MS-, and TS-porins in the presence of a variety of KCl-concentrations. Surprisingly, the single-channel conductance of TS-porin was not a linear function of the bulk aqueous salt concentration, as has been found previously for the native porin (Benz et al., 1987) and still is approximately the case for the MS-porin. Instead, we observed that the conductance followed the square root of the concentration with an approximate slope of 0.5 on a double logarithmic scale (Table 2; Fig. 9). This result suggested negative surface charge effects on ion transport through the TS-porin channel. Similar negative surface charge effects have been found previously for the hemolysine channels of *E. coli* and other related bacteria (Benz et al., 1989, 1994; Ropele & Menestrina, 1989), and for porins from *Pelobacter*

Table 2. *Average single-channel conductance (G) of native porin, MS-porin, and TS-porin R. capsulatus in different salt solutions*

			G (nS)	
Salt	c (M)	Native porin	MS-porin	TS-porin
LiCl	1	1.3 ± 0.11	1.3 ± 0.10	1.0 ± 0.10
KCl	0.01	0.030 ± 0.003	0.090 ± 0.001	0.30 ± 0.05
	0.03	0.095 ± 0.01	0.24 ± 0.003	0.53 ± 0.062
	0.10	0.32 ± 0.035	0.50 ± 0.045	0.90 ± 0.085
	0.30	1.00 ± 0.01	1.10 ± 0.13	1.45 ± 0.25
	1.0	2.90 ± 0.31	2.60 ± 0.27	3.30 ± 0.30
	3.0	7.4 ± 0.73	6.0 ± 0.55	6.5 ± 0.58
KCH_3COO (pH 7)	1.0	2.0 ± 0.22	2.2 ± 0.30	2.7 ± 0.22

Note: The membranes were formed of diphytanoyl phosphatidylcholine dissolved in n-decane. The aqueous solutions were unbuffered and had a pH of 6 unless otherwise indicated. The applied voltage was 20 mV, and the temperature was 20 °C. The average single-channel conductance G was claculated from at least 80 single events; c is the concentration of the aqueous salt solutions. See Fig. 8 for standard deviation at 0.3 M KCL.

venetianus (Schmid et al., 1991) and *Acidovorax delafildii* (Brunen et al., 1991). Single-channel experiments were also performed with salts other than KCl to obtain information on the selectivity of the TS-porin. These results (see Table 2) showed that replacement of chloride by the less mobile acetate had only little influence on the conductance of the TS-porin. The influence of the cations on the single-channel conductance was more pronounced (Table 2), suggesting that the TS-porin is cation selective, as has been observed for the native porin (Benz et al., 1987).

Selectivity of the succinylated porin

Zero-current membrane potential measurements were performed to obtain further information on the ion permeabilities of the TS-porin. Membranes of diphytanoyl phosphatidylcholine/*n*-decane were formed in 10-mM salt solutions, and MS-porin and TS-porin were added to the aqueous phase when the membranes were in the black state. After incorporation of 100–1,000 channels into a membrane, 10-fold salt gradients were established by addition of small amounts of concentrated salt solution to one side of the membrane. For all salts (KCl, LiCl, and KCH_3COO) tested in these experiments, the more diluted side of the membrane became positive, which indicated preferential movement of cations through the MS- and TS-porin channels, i.e., the channels are cation-selective, as suggested from the single-channel data (see Table 3). The zero-current membrane potential was 44 and 49 mV with KCl for MS-porin and TS-porin, respectively, compared with 39 mV for the unmodified porin.

Analysis of the zero-current membrane potential in Table 3 using the Goldman-Hodgkin-Katz equation (Benz et al., 1985) suggested that anions also could have a certain permeability through the TS-porin channels because the ratios of the permeabilities P_{cation} and P_{anions} were between 21 and 23. On the other hand, the asymmetry potentials were very similar for the three salts composed of anions and cations of different mobilities, which is not expected for a general diffusion pore (Benz et al., 1985). The ratios of permeabilities P_{cation}, P_{anion} were between 7 and 15 for the native porin channel, and increased significantly for the three different salts on succinylation (see Table 3). This suggested that the MS-porin and TS-porin had become substantially more selective for cations because of point charges attached to the channel (see below and Discussion). This change in selectivity must be due to the amino-succinylated residues identified, i.e., conversion of Lys-46 and the N-terminus into negatively charged groups in the case of the MS-porin, and of Lys-46, Lys-298, Lys-300, and the N-terminus for the TS-porin.

Structure of the TS-porin

The TS-porin from *R. capsulatus* 37b4 crystallized in space group R3 under similar conditions as native porin from this strain. The unit cell constants of native and TS-porin crystals were $a = b = 92.0$ Å and 91.7 Å, and $c = 145.9$ Å and 145.7 Å, respectively. The structure was analyzed with difference Fourier electron density maps using the known structure of the native porin (see Materials and methods and Table 4). Crystals of TS-porin diffracted to 2.4 Å; data were evaluated to 2.7 Å.

Positive electron density, as revealed by $2F_{obs} - F_{calc}$ density maps, was found near four ϵ-amino groups of the ten lysine residues: Lys-46, Lys-69, Lys-230, and Lys-300. Of these residues, only Lys-46 and Lys-300 (both located on the inner channel surface) were identified by mass spectrometry as succinylation sites. By contrast, Lys-69, albeit on the inner channel surface, was found unsuccinylated (or modified only to a very low extent), which can be explained by the considerable shielding of this

Table 3. *Zero-current membrane potentials (V_m) of diphytanoyl phosphatidyl-choline/n-decane membranes in the presence of native porin, MS-porin, and TS-porin of R. capsulatus measured for a 10-fold gradient of different salts*

	V_m (mV)	P_{cation}/P_{anion}
Native porin		
KCl	39 ± 2.0	9.0 ± 1.0
LiCl	36 ± 1.6	7.0 ± 0.5
K-acetate (pH 7)	45 ± 2.2	15 ± 1.2
MS-porin		
KCl	44 ± 1.4	13 ± 1.4
TS-porin		
KCl	49 ± 1.5	23 ± 1.5
LiCl	48 ± 2.0	21 ± 2.0
K-acetate (pH 7)	49 ± 1.3	22 ± 1.8

Note: V_m is defined as the difference between the potential at the dilute side (10 mM) and the potential at the concentrated side (100 mM). The pH of the aqueous salt solutions was 6 unless otherwise indicated; T = 20 °C. The permeability ratio P_{cation}/P_{anion} was calculated with the Goldman-Hodgkin-Katz equation (Benz et al., 1985) on the basis of at least three individual experiments.

Table 4. *Refined structure of TS-porin from R. capsulatus 37b4*

Resolution 10–2.7 Å	
No. reflections	12,289
Completeness	97.2%
Internal R-value on Intensities	8.8%
Crystallographic free R-value	20.8%
Crystallographic working R-value	19.9%
RMS	
Bond lengths (Å)	0.009
Bond angles (deg.)	1.6
Dihedral angles (deg.)	27.9
Improper angles (deg.)	1.2
No. non-hydrogen atoms	
Polypeptide	2,219
Water	259
Detergent	42
Calcium	4
Average B-factors (Å^2)	
All atoms	23
Polypeptide atoms	22
Main chain atoms	18
Side chain atoms	25
Water molecules	38
Detergent molecules	58

ϵ-amino group by the adjacent Phe-62 and Glu-71 residues (Weiss & Schulz, 1992). Contiguous density of sufficient volume to harbor a succinyl group was found only near Lys-46. Refinement was done after introducing the N-ϵ-(succinyl)-Lys-46 (see details in Table 4), yielding a final R-factor of 19.9%. The $2F_{obs} - F_{calc}$ density of succinyl-lysine-46 is shown in Figure 10.

Stereo views of the Cα-chain of TS-porin, the succinylated residues Lys-46, Lys-300, Lys-298, Glu-1(α-NH_2), and the unmodified inner channel and outer surface Lys residues are shown in Figure 11A and B. The structural comparison with native porin revealed that all succinylated lysine residues are located at the inner channel surface and are solvent-accessible, i.e., not shielded by neighboring groups: Lys-46 is located at the channel constriction site, whereas the other succinylated residues Lys-300, Lys-298, and the N-terminus are all near the periplasmic pore mouth. Of the further Lys residues at the inner surface (Lys-3, Lys-69, Lys-191, Lys-198), a low to trace extent of modification was found only for Lys-3 and Lys-69. Lys-69 is shielded by the adjacent Phe-62 and Glu-71 residues, Lys-191 by Asn-196, and Lys-198 is shielded within 4 Å by the Phe-83 and Asp-85 residues. These results are in agreement with the previously established predominant reactivity of free surface accessible lysine residues toward amino acylation (Glocker et al., 1994). Three other lysine residues (Lys-138, Lys-169, Lys-230) on the outer surface of the barrel are not succinylated, which can be explained by shielding due to surrounding detergent molecules (Weiss et al, 1991a). The low reactivity of the Lys-3 residue at the inner channel surface toward succinylation can be explained by shielding due to the Ser-5 and Thr-30 residues, and by a local conformational change that may occur on succinylation of the adjacent N-terminal (Glu-1)-amino group (Suckau et al., 1992; Glocker et al., 1994).

The side chain of Lys-46 originally pointed almost horizontally toward the center of the opposite third external loop. On succinylation, it bends toward the periplasmic surface. The attached 3-carboxypropionyl group bends further in this direction and to the right when seen along the membrane normal toward the external phase. The average angle of the succinyl-lysine side chain with the membrane is approximately 35 degrees. The terminal carboxyl group shows no polar interactions with protein residues. Because no electron density was observed for the succinylated Lys-300, Lys-298, and the N-terminal amino groups in the difference map, at the periplasmic entrance of the channel a considerable disorder must be assumed for these succinyl groups.

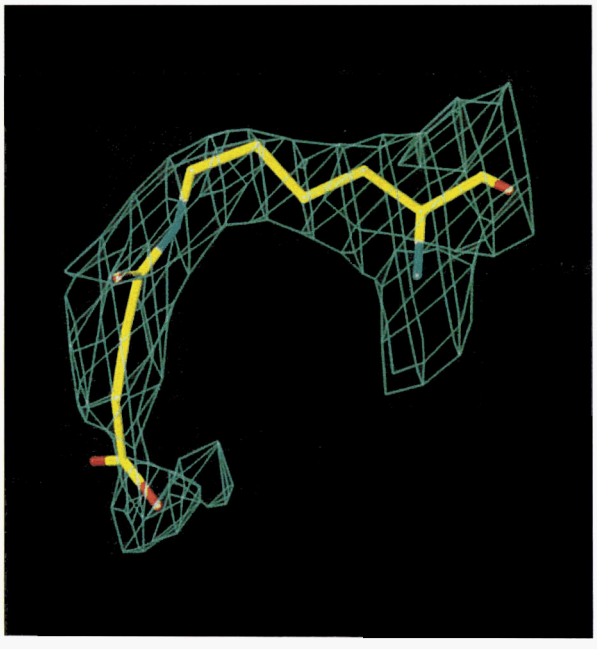

Fig. 10. $2F_{obs} - F_{calc}$ density and model of succinylated lysine-46 residue. The density is plotted at a 1σ level.

Discussion

The electrical properties of porin from *R. capsulatus* were substantially modified on succinylation. The observed changes are in complete agreement with the specific succinylation sites identified: all of the succinylated amino groups are solvent-accessible and are located at critical positions for the passage of ions (see Fig. 11). In contrast to the other, native charged side chains in this region, the structure of succinyl-lysine-46 as modeled from the electron density map does not point in extended conformation toward the opposite segment of the constriction site, but bends toward the periplasmic space. Thereby, the succinyl-carboxylate group is located distant from the negatively charged Asp and Glu residues on the opposite segment of the constriction site. No evident attractive electrical interactions favor this conformation.

In spite of the bulky amino-succinylated residues, the succinylation increased the single-channel conductance (see Fig. 8). Moreover, the single-channel conductance of the TS-porin was no longer a linear function of the bulk aqueous concentration (see Table 2). Instead, a slope of approximately 0.5 to 0.6 was observed on a double-logarithmic scale for the conductance-versus-concentration curve, indicating that negative surface charge effects determine the properties of the TS-porin channel (Menestrina & Antolini, 1981). In addition to the succinylated Lys-46 residue in the channel eyelet, the negative charges introduced by the modification of the Lys-298, Lys-300 residues, and the N-terminus are all located near the periplasmic pore mouth, resulting in substantial ionic strength-dependent surface potentials that attract cations and repel anions. Accordingly, they are expected to influence both the single-channel conductance and zero-current membrane potential.

A quantitative description of the effect of the point charges introduced at the channel eyelet and the pore mouth on the single-channel conductance may be given on the basis of the following consideration. The surface potential, Φ for a channel with radius r, and a total charge q (in As), is given by (Nelson & McQuarrie, 1975; Menestrina & Antolini, 1981):

$$\Phi = 2 \cdot q \exp(-r/l_D)/(4 \cdot \pi \cdot \epsilon_0 \cdot \epsilon \cdot r), \quad (1)$$

where $\epsilon 0$ ($= 8.85 \times 10^{-12} F/m$) and ϵ ($= 80$) are the absolute dielectric constants of vacuum and the relative dielectric constant of water, respectively, and l_D is the so called Debeye length, which controls the decay of the potential (and of the accumulated positively charged ions) in the aqueous phase:

$$l_D^2 = \epsilon \cdot \epsilon_0 \cdot R \cdot T/(2 \cdot F^2 \cdot c), \quad (2)$$

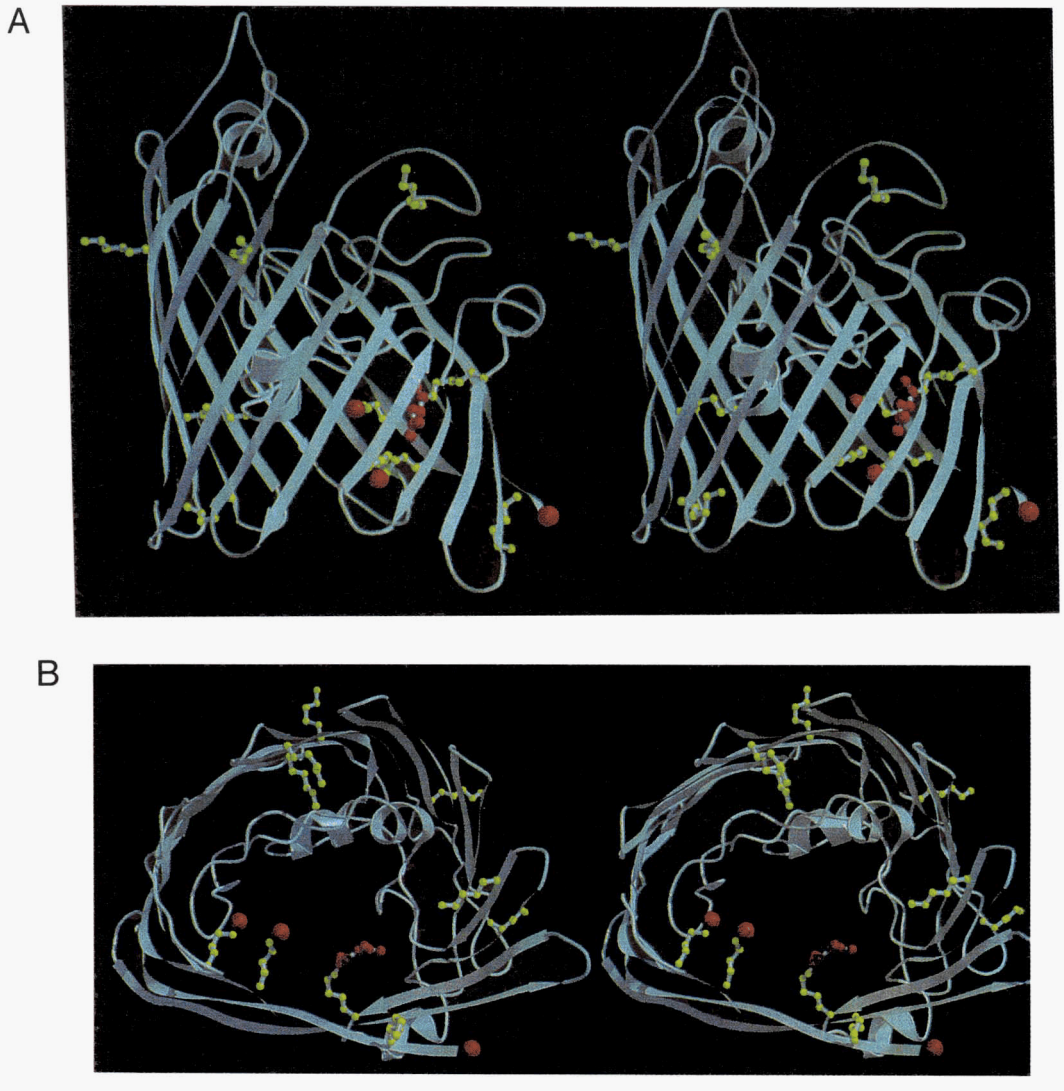

Fig. 11. Stereo views of Cα-chain in ribbon representation and distribution of lysine residues in the TS-porin channel. All lysine residues are depicted in yellow. Succinylated lysine residues are indicated by a red sphere at the position of the ϵ-amino group. For the succinylated Lys-46 residue, the structure derived from the X-ray analysis is shown. **A:** View along the membrane normal from the external side. **B:** View parallel to the membrane.

with c = bulk aqueous salt concentration; and $RT/F = 25.2$ mV at 20 °C. Values for l_D calculated for different ion concentrations using Equation 2 are given in Table 5. As shown in Figure 9, particularly for TS-porin with the additional succinylation sites at the pore mouth, the single-channel conductance differs from that of native porin as long as the Debeye length is definitely larger than the radius of the channel eyelet. This contrasts with the smaller effect observed for MS-porin on succinylation of the inner-channel Lys-46 residue. Because porin channels are present in the black lipid film at very low density, the negative charges of the succinyl groups at Lys-298, Lys-300, and the N-terminus at low ionic strength can act as a funnel, helping to direct cations from the bulk solution into the channel mouth. The more charges are accumulated there, the higher the channel conductance should be in comparison to the native protein. The concentration of monovalent cations (c_0^+) at the channel mouth is given by:

$$c_0^+ = c \cdot \exp(-\Phi \cdot F/(R \cdot T)). \quad (3)$$

The cation concentration c_0^+ at the pore mouth can now be used for the calculation of the effective conductance concentration curve $G(c)$:

$$G(c) = G_0 \cdot c_0^+. \quad (4)$$

Table 5. *Debeye length calculated with Equation 2 for a single elementary charge and different concentrations of a monovalent salt in water at room temperature*

c	1 mM	10 mM	0.1 M	1 M
l_D	96 Å	30 Å	9.6 Å	3 Å

A best fit of the data in Table 3 was obtained by assuming a negative elementary charge of 1.0 for TS-porin and of 0.6 for MS-porin located at the pore mouth, and a radius of approximately 0.5 nm for both succinylated proteins. This can be shown by a fit of the single-channel conductance as a function of the bulk aqueous concentration c by Equation 4, which represents a combination of Equations 1–3 (see Fig. 9). The fit yielded a value of G_0 of 2.0 nS/M, which corresponds to a single-channel conductance G in the absence of the point charges of 2.0 nS at 1 M Kcl. The single-channel conductance G_0, in the absence of the point charges, was assumed to be 2.0 nS. It is noteworthy that the number of negatively charged groups involved in the point charges is somewhat tentative because two different formalisms—the Debeye-Hückel theory and the treatment by Nelson and McQuarrie (1975)—can be applied to the problem. Both differ in the number of charges by a factor of two, because a charge at the surface of a low dielectric membrane induces an image charge on the opposite side. On the other hand, the dielectric constant of a membrane protein is neither 2 nor 80, which means that the number of charges will be intermediate between 1, according to the Nelson-McQuarrie treatment, and 2, according to the Debye-Hückel treatment (see Benz et al., 1994 for a more complete discussion of this problem).

Formally, eight negative charges were introduced in TS-porin by succinylation of four amino groups. However, only one to two negative charges are needed to explain the point charge effect on the single-channel conductance. This difference may be due to neutralization effects, pK differences, and steric effects, which all limit the validity of the above theoretical treatment and lead obviously to a reduction of the apparent number of negatively charged groups compared with the theoretically possible ones. Furthermore, we must consider the possibility that some of the eight additional negative charges counterbalance with the other positive charges present in the channel.

The ion selectivity in the succinylated porins shifted, as expected due to the replacement of up to four amino groups by negatively charged succinate groups. As indicated by the increase of the P_{cation}/P_{anion} ratio, succinylation facilitates the cation relative to anion permeability, consistent with previous studies of chemically modified *E. coli* B-porins (Tokunaga et al., 1981; Benz et al., 1984) and of PhoE mutants using single-site amino acid substitutions (Bauer et al., 1989). These results are consistent with the model that the loop segment folded into the β-barrel interior containing acidic side chains determines the cation permeability and, vice-versa, that the basic residues of the opposite segment are responsible for the anion permeability. Tertiary structure-selective chemical modification such as by lysine-succinylation in this study, characterized by mass spectrometric peptide mapping, provides an efficient method for understanding electrical properties of channel proteins (Przybylski et al., 1993; Przybylski & Glocker, 1996).

Among channel proteins, general-diffusion porins are characterized by their large and rather nonspecific single-channel conductance. Although sodium and potassium channel conductances range from 2 to 50 pS (Hille, 1991), general-diffusion porin monomers at similar conditions range between 500 and 1,000 pS (Benz & Bauer, 1988). Moreover, the former channels show flux saturation (Sakmann & Trube, 1984) and have been modeled as a sequence of energy barriers connected by binding sites (Lauger, 1973; Dani, 1986). In contrast, even the simple symmetrical two-barrier-one-site model does not appear to be justified for the general diffusion porins with a linear relation between conductance and ion concentration, which can only be described by a one-barrier model.

The present study provides evidence that in the TS-porin negative charges are placed directly at the periplasmic channel mouth of porin. The single-channel conductance is then no longer linear, but shows saturation and resembles a square-root function, concomitant with an increased selectivity for cations. This effect of charges near the channel mouth has been predicted by Menestrina and Antolini (1981), Dani (1986), and Jordan (1987) for ion channels in general, and has been verified experimentally in a Ca^{++}-activated K^+-channel by chemical modification of surface carboxylate groups (MacKinnon et al., 1989). Strategically placed charges near the periplasmic channel mouth can thus both lower energy barriers inside the channel and act as funnels to guide ions into the mouth. In this manner, the selective amino-succinylation shown here can provide the satisfaction of the two contradictory requirements of many ion channels: high selectivity *and* high conductivity.

Materials and methods

Growth and purification of porin

R. capsulatus 37b4 cells were grown and harvested as described (Nestel et al., 1989). Porin was purified according to Kreusch et al. (1991).

Succinylation of porin

The succinylation of porin was carried out essentially as described previously (Tokunaga et al., 1981; Glocker et al., 1994). The reaction was started by diluting a protein stock solution (6 mg/mL) to 1 mg/mL and pipetting a 500-μL aliquot to different amounts of succinic anhydride (0.2 and 1.4 mg, respectively), and the pH kept at 6.5 for 60 min with a pH-stat by automated addition of a 1-M NaOH solution. Succinylated protein was dialyzed against 20 mM tris(hydroxymethyl)aminomethane, 300 mM LiCl, 3 mM NaN3 containing 0.6% (w/v) *n*-octyltetraoxyethylene (crystallization buffer) and finally purified by FPLC (fast-flow Q-sepharose; Pharmacia, Freiburg, Germany).

Proteolytic degradation and HPLC isolation of peptide fragments

BrCN degradation of native and succinylated porin was performed with protein samples of 100 μg (approximately 3 nmol). Protein solutions in 10 μL crystallization buffer (20 mM NaN_3 with 0.6% *n*-octyltetraoxyethylene) were mixed with 25 μL 70% formic acid and 15 μmol (5 M solution in acetonitrile) BrCN added under a continuous N_2-stream. Degradation was performed for 24 h at 20 °C in subdued light, and the reaction quenched by addition of 1 mL H_2O. A 1-μL aliquot was used directly for MALDI-MS peptide mapping analysis, and the remaining peptide fragment mixture subjected to HPLC separation.

Tryptic digestion was performed with solutions of 60 μg native porin and the succinylated porin derivatives in 6 μL crystallization buffer that was mixed with 51 μL of a 2 M urea solution in H_2O and denatured for 5 min at 95 °C. The solution was cooled to room temperature, brought to pH 8 by addition

of 60 μL 100 mM NH_4HCO_3, and digested for 4 h (37 °C) with 3 μg trypsin (Sigma; untreated in 1 mM HCl or TPCK-treated).

HPLC separations of peptide fragments were performed with a Waters-Millipore M-590/510 solvent delivery instrument/M-490 UV detection system. One-hundred-microliter aliquots of tryptic digest mixtures were separated on a 25 × 0.4-cm C8-nucleosil column (Macherey-Nagel, Duisburg, Germany), using a linear binary gradient of 0.04% aqueous TFA (A) and 0.03% TFA in acetonitril (B), 5–95% B/60 min. A 20 × 0.4-cm C4-nucleosil column was used for the separation of BrCN peptides, at otherwise identical conditions. Peptide fractions were isolated with a Gilson-CPR fraction collector and used directly for mass spectrometric analysis or blotted to PVDF membranes for sequence determinations. Edman sequence analyses were performed on a Knauer 910 automated sequencer.

Mass spectrometry

MALDI-MS was performed with a Bruker Biflex time-of-flight spectrometer (Bruker-Franzen, Bremen, Germany) equipped with a UV-nitrogen laser (337 nm) and a dual channel plate detector and *x*-mass data system for spectra acquisition and instrument control. Sample preparation was conducted with 1-μL solutions of porin and succinylated porin derivatives in crystallization buffer (10 μg/μL), which were mixed with 19 μL of a solution (23 μg/μL) of the matrix HCCA in acetonitril:0.1% TFA (2:1). A 1-μL aliquot of the resulting solution spotted on a 3-mm^2 stainless steel target was brought to dryness within 3–4 min at room temperature. The crystalline sample/matrix preparation was then controlled by a microscope and inserted into the ion source. Spectra were obtained with an acceleration voltage of 10 kV, approximately $5 \cdot 10^6$ W/cm^2 laser power, and 10 Hz pulse frequency (3 ns).

Spectra of proteolytic digest mixtures and isolated peptide fragments were obtained with the same solvent conditions, using 1:1-mixtures of sample:matrix solutions.

Crystallization

Crystallization was conducted at 17 °C using the sitting-drop method. Protein concentration in the drop was 5 mg/mL in a buffer containing crystallization buffer and 8% (w/v) of the precipitating agent PEG-600. The concentration of the precipitant in the reservoir solution was 35% (w/v). The best crystals were of perfect rhombohedral habit and grew in two weeks to a maximum size of 300 × 300 × 300 μm. The space group was R3.

Data collection

X-ray diffraction data to 2.4 Å resolution were collected at room temperature on an image plate detector (STOE, Darmstadt) mounted on a rotating anode X-ray generator (Siemens). The raw data were processed with the program XDS (Kabsch, 1988). The 28·762 independent intensity measurements were reduced to 15·652 in the resolution range ∞–2.4 Å, showing an overall R_{sym} of 10.6% on intensities. The overall completeness of the data set was 85.8% and 97.2% in the resolution shell ∞–2.7 Å. Because the R_{sym} on intensities in the outermost resolution shell (2.4–2.7 Å) was 37.3%, only the reflections from ∞ to 2.7 Å with an overall R of 8.8% on intensities were used. The hexagonal axes were determined as $a = b = 91.7$ Å and $c = 145.7$ Å.

Refinement

The structure solution was initiated with the refined model of the native crystal form "C" (unpubl. data) containing four calcium atoms, two detergent molecules, and 268 water molecules. The subunit location was adjusted by 11 cycles of rigid body refinement at 2.7 Å resolution using the program X-PLOR (Brünger, 1988). The resulting eulerian rotation angles (Θ1, Θ2, Θ3) were −0.02 degree, 0.01 degree, 0.19 degree and the translation was −0.01 Å, 0.09 Å, 0.00 Å.

For refinement of the succinyl-lysine, partial charges were set to zero. The corresponding $2F_{obs} - F_{calc}$-map showed that for six of the ten lysine residues no electron density adjacent to their side chain. Three lysine residues (Lys-69, Lys-230, Lys-300) had some density at the ε-nitrogen, but not sufficient for fitting a ε-N-(succinyl)-lysine. Only for Lys-46 contiguous density of sufficient volume was found. For the refinement, all other atoms except those of succinyl-Lys-46 were fixed. After 40 cycles of conjugate gradient minimization, 20 cycles of temperature factor refinement, and an occupancy refinement for only the succinyl-Lys-46, a final free R-value (Brünger, 1993) of 20.8% and a final working R-value of 19.9% was obtained, respectively.

The figures were prepared with the program O (Jones et al., 1991) on a Silicon Graphics 4D210 VGX computer.

Lipid bilayer experiments

The methods used for the "black" lipid bilayer experiments have been described previously (Benz et al., 1985). Membranes were formed from a 1% (w/v) solution of diphytanoyl phosphatidylcholine (DiphPC, Avanti Polar Lipids, Alabaster, Alabama) in *n*-decane across circular holes (surface area approximately 0.5–1 mm^2) in the thin wall of a Teflon cell separating the two aqueous compartments. The temperature was kept at 25 °C. All salts and buffers were of analytical grade and obtained from Merck (Darmstadt, Germany). The aqueous solutions were either unbuffered (ca. pH 6), or buffered with 10 mM Hepes to pH 7. Native porin and succinylated protein derivatives were added from the stock solutions to the aqueous phase of the *cis* compartment (compartment to which the voltage was applied) after the membranes had turned optically black in reflected light. The current through the membranes was measured with two calomel electrodes switched in series with a voltage source and a model 427 current amplifier (Keithley, Cleveland, Ohio). The amplified signal was monitored with a storage oscilloscope and recorded on a strip chart recorder. For macroscopic conductance measurements, the current amplifier was replaced by a Keithley electrometer (model 602). Zero-current membrane potentials were measured with the same instrument 5–10 min after the application of a salt gradient across the membrane (Benz et al., 1979).

Acknowledgments

This work was supported by the Deutsche Forschungsgemeinschaft (Sonderforschungsbereich 176; We962 and Pr175), Fonds der Chemischen Industrie, and by the EU-network "Peptide and Protein Structure Elucidation by Mass Spectrometry." We thank Dr. D. Suckau and Dr. U. Rapp (Bruker-Franzen, Bremen) for help and assistance with the MALDI-MS instrumentation, and Dr. P. Hojrup (Odense University, Denmark) for help with the Edman sequence determinations.

References

Bauer K, Struyve M, Bosch D, Benz R, Tommassen J. 1989. One single lysine-residue is responsible for the special interaction between polyphosphate and the outer membrane porin PhoE of *Escherichia coli*. *J Biol Chem 264*:16393–16398.

Benz R. 1988. Structure and function of porins from Gram-negative bacteria. *Annu Rev Microbiol 42*:359–393.

Benz R, Bauer K. 1988. Permeation of hydrophilic molecules through the outer membrane of Gram-negative bacteria. *Eur J Biochem 176*:1–19.

Benz R, Hardie KR, Hughes C. 1994. Pore-formation in artificial membranes by the secreted hemolysins of *Proteus vulgaris* and *Morganella morganii*. *Eur J Biochem 220*:339–347.

Benz R, Janko K, Lauger P. 1979. Ionic selectivity of pores formed by the matrix protein porin of *Escherichia coli*. *Biochim Biophys Acta 551*: 238–247.

Benz R, Schmid A, Hancock REW. 1985. Ion selectivity of Gram-negative bacterial porins. *J Bacteriol 162*:722–727.

Benz R, Schmid A, Wagner W, Goebel W. 1989. Pore formation by the *Escherichia coli* hemolysin: Evidence for an association–dissociation equilibrium of the pore-forming aggregates. *Infect Immun 57*:887–895.

Benz R, Tokunaga H, Nakae T. 1984. Properties of chemically modified porin from *Escherichia coli* in lipid bilayer membranes. *Biochim Biophys Acta 769*:348–356.

Benz R, Woitzik D, Flammann HT, Weckesser J. 1987. Pore forming activity of the major outer membrane protein of *Rhodobacter capsulatus* in lipid bilayer membranes. *Arch Microbiol 14*:226–230.

Brunen M, Engelhardt H, Schmid A, Benz R. 1991. The major outer membrane protein of *Acidovorax delafieldii* is an anion-selective porin. *J Bacteriol 173*:4182–4187.

Brünger AT. 1988. Crystallographic refinement by simulated annealing: Application to a 2.8 Å resolution structure of aspartate aminotransferase. *J Mol Biol 203*:80.

Brünger AT. 1993. Assessment of phase accuracy by cross validation: The free *R* value. Methods and applications. *Acta Crystallogr D 49*:24–36.

Cowan SW, Schirmer T, Rummel G, Steiert M, Ghosh R, Pauptit RA, Jansonius JN, Rosenbusch JP. 1992. Crystal structures explain functional properties of two *E. coli* porins. *Nature 358*:727–733.

Dani JA. 1986. Ion-channel entrances influence permeation. *Biophys J 49*:607–618.

Fontana A, Gross E. 1986. Fragmentation of polypeptides by chemical methods. In: Darbre A, ed. *Practical protein chemistry—A handbook*. Chichester: John Wiley & Sons. pp 83–88.

Glocker MO, Borchers C, Fiedler W, Suckau D, Przybylski M. 1994. Molecular characterization of surface topology in protein tertiary structures by amino-acylation and mass spectrometric peptide mapping. *Bioconj Chem 5*:583–591.

Hille B. 1991. *Ionic channels of excitable membranes*. Sunderland, Massachusetts: Sinauer Assoc. Inc.

Jones TA, Zou JY, Cowan SW, Kjeldgaard M. 1991. Improved methods for building protein models in electron density maps and the location of errors in these models. *Acta Crystallogr A 47*:110–119.

Jordan PC. 1987. How pore mouth charge distributions alter the permeability of transmembrane ionic channels. *Biophys J 51*:297–311.

Kabsch W. 1988. Automatic indexing of rotation diffraction patterns. *J Appl Crystallogr 21*:67–71.

Karas M, Bahr U, Gießmann U. 1991. Matrix-assisted laser desorption ionization mass spectrometry. *Mass Spectrom Rev 10*:335–358.

Kreusch A, Neubuser A, Schiltz E, Weckesser J, Schulz GE. 1994. Structure of the membrane channel porin from *Rhodopseudomonas blastica* at 2.0 Å resolution. *Protein Sci 3*:58–63.

Kreusch A, Weiss MS, Welte W, Weckesser J, Schulz GE. 1991. Crystals of an integral membrane protein diffracting to 1.8 Å resolution. *J Mol Biol 217*:9–10.

Lauger P. 1973. Ion transport through pores: A rate-theory analysis. *Biochim Biophys Acta 311*:423–441.

MacKinnon R, Latorre R, Miller C. 1989. Role of surface electrostatics in the operation of a high-conductance Ca^{++}-activated K^+ channel. *Biochemistry 28*:8092–8099.

Menestrina R, Antolini R. 1981. Ion transport through hemocyanin channels in oxidised cholesterol membranes. *Biochim Biophys Acta 643*:616–625.

Nelson AP, McQuarrie DA. 1975. The effect of discrete charges on the electrical properties of a membrane. *J Theor Biol 55*:13–27.

Nestel U, Wacker T, Woitzik D, Weckesser J, Kreutz W, Welte W. 1989. Crystallization and preliminary X-ray analysis of porin from *Rhodobacter capsulatus*. *FEBS Lett 242*:405–408.

Nielsen PF, Schneider K, Suckau D, Landis B, Przybylski M. 1990. Applications of selective chemical reactions in combination with 252-californium plasma desorption mass spectrometry in protein structure analysis. In: Hilf E, ed. *Mass spectrometry of large non-volatile molecules, vol 3*. London: World Scientif. pp 194–207.

Przybylski M. 1995. Mass spectrometric approaches to the characterization of tertiary and supramolecular structures of biomacromolecules. *Adv Mass Spectrom 13*:257–285.

Przybylski M, Borchers C, Suckau D, Mák M, Jetschke M. 1993. Selective chemical modification and mass spectrometric peptide mapping: A new approach for the molecular characterization of surface topology and micro-environment in protein tertiary structures. In: Schneider CH, Eberle AN, eds. *Peptides 1992*. Amsterdam: Escom Science Publ. pp 915–916.

Przybylski M, Glocker MO. 1996. Electrospray mass spectrometry of noncovalent complexes of biomacromolecules—New analytical perspectives for supramolecular chemistry and molecular recognition processes. *Angew Chem Int Ed Engl. 35*:806–826.

Rietschel ET, Brade L, Schade U, Seydel U, Zähringer U, Kusumoto S, Brade H. 1988. Bacterial endotoxins: Properties and structure of biologically active domains. In: Schrinner E, Richmond MH, Seinbert G, Schwarz U, eds. *Surface structures of microorganisms and their interactions with the mammalian host*. pp 1–41.

Ropele M, Menestrina G. 1989. Electrical properties and molecular architecture of the channel formed by *Escherichia coli* hemolysin in planar lipid membranes. *Biochim Biophys Acta 985*:9–18.

Sakmann B, Trube G. 1984. Voltage-dependent inactivation of inward-rectifying single-channel currents in the guinea-pig heart cell membrane. *J Physiol 347*:659–683.

Schiltz E, Kreusch A, Nestel U, Schulz GE. 1991. Primary structure of porin from *Rhodobacter capsulatus*. *Eur J Biochem 199*:587–594.

Schirmer T, Keller TA, Wang YF, Rosenbusch JP. 1995. Structural basis for sugar translocation through maltoporin channels at 3.1 Å resolution. *Science 267*:512–514.

Schmid A, Benz R, Schink B. 1991. Identification of two porins in *Pelobacter venetianus* fermenting high molecular mass polyethylene glycols. *J Bacteriol 173*:4909–4913.

Smith RD, Loo JA, Orgorzalek Loo RR, Busman M, Udseth HR. 1991. Principles and practice of electrospray ionization-mass spectrometry for large polypeptides and proteins. *Mass Spectrom Rev 10*:359–401.

Suckau D, Mák M, Przybylski M. 1992. Protein surface topology probing by selective chemical modification and mass spectrometric peptide mapping. *Proc Natl Acad Sci USA 89*:5630–5634.

Tokunaga H, Tokunaga M, Nakae T. 1981. Permeability properties of chemically modified porin trimers from *Escherichia coli* B. *J Biol Chem 256*: 8024–8029.

Weiss MS, Abele U, Weckesser J, Welte W, Schiltz E, Schulz GE. 1991a. Molecular architecture and electrostatic properties of a bacterial porin. *Science 254*:1627–1630.

Weiss MS, Kreusch A, Schiltz E, Nestel U, Welte W, Weckesser J, Schulz GE. 1991b. The structure of porin from *Rhodobacter capsulatus* at 1.8 Å resolution. *FEBS Lett 280*:379–382.

Weiss MS, Schulz GE. 1992. Structure of porin refined at 1.8 Å resolution. *J Mol Biol 227*:493–509.

Welte W, Nestel U, Wacker T, Diederichs K. 1995. Structure and function of the porin channel. *Kidney International 48*:930–940.